Comparison of a multileaf collimator tracking system and a robotic treatment couch tracking system for organ motion compensation during radiotherapy

Martin J. Menten[a)]
Department of Medical Physics in Radiation Oncology, German Cancer Research Center, Im Neuenheimer Feld 280, D-69120 Heidelberg, Germany

Matthias Guckenberger
Department of Radiation Oncology, University of Würzburg, Josef-Schneider-Straße 11, D-97080 Würzburg, Germany

Christian Herrmann
Department of Computer Sciences VII, Robotics and Telematics, University of Würzburg, Am Hubland, D-97074 Würzburg, Germany

Andreas Krauß, Simeon Nill, and Uwe Oelfke
Department of Medical Physics in Radiation Oncology, German Cancer Research Center, Im Neuenheimer Feld 280, D-69120 Heidelberg, Germany

Jürgen Wilbert
Department of Radiation Oncology, University of Würzburg, Josef-Schneider-Straße 11, D-97080 Würzburg, Germany

(Received 1 June 2012; revised 29 September 2012; accepted for publication 2 October 2012; published 29 October 2012)

Purpose: One limitation of accurate dose delivery in radiotherapy is intrafractional movement of the tumor or the entire patient which may lead to an underdosage of the target tissue or an overdosage of adjacent organs at risk. In order to compensate for this movement, different techniques have been developed. In this study the tracking performances of a multileaf collimator (MLC) tracking system and a robotic treatment couch tracking system were compared under equal conditions.
Methods: MLC tracking was performed using a tracking system based on the Siemens 160 MLC. A HexaPOD robotic treatment couch tracking system was also installed at the same linac. A programmable 4D motion stage was used to reproduce motion trajectories with different target phantoms. Motion localization of the target was provided by the 4D tracking system of Calypso Medical Inc. The gained positional data served as input signal for the control systems of the MLC and HexaPOD tracking systems attempting to compensate for the target motion. The geometric and dosimetric accuracy for the tracking of eight different respiratory motion trajectories was investigated for both systems. The dosimetric accuracy of both systems was also evaluated for the tracking of five prostate motion trajectories.
Results: For the respiratory motion the average root mean square error of all trajectories in y direction was reduced from 4.1 to 2.0 mm for MLC tracking and to 2.2 mm for HexaPOD tracking. In x direction it was reduced from 1.9 to 0.9 mm (MLC) and to 1.0 mm (HexaPOD). The average 2%/2 mm gamma pass rate for the respiratory motion trajectories was increased from 76.4% for no tracking to 89.8% and 95.3% for the MLC and the HexaPOD tracking systems, respectively. For the prostate motion trajectories the average 2%/2 mm gamma pass rate was 60.1% when no tracking was applied and was improved to 85.0% for MLC tracking and 95.3% for the HexaPOD tracking system.
Conclusions: Both systems clearly increased the geometric and dosimetric accuracy during tracking of respiratory motion trajectories. Thereby, the geometric accuracy was increased almost equally by both systems, whereas the dosimetric accuracy of the HexaPOD tracking system was slightly better for all considered respiratory motion trajectories. Substantial improvement of the dosimetric accuracy was also observed during tracking of prostate motion trajectories during an intensity-modulated radiotherapy plan. Thereby, the HexaPOD tracking system showed better results than the MLC tracking. [http://dx.doi.org/10.1118/1.4761868]

Key words: MLC, couch tracking, Calypso

I. INTRODUCTION

In the ongoing struggle to treat cancer, radiotherapy is one of the most commonly used tools besides chemotherapy and surgery. The goal of modern radiotherapy is the delivery of a sufficient dose of high-energy radiation to the tumor in order to achieve the desired therapeutic effect, while sparing as much healthy tissue as possible. Conformal radiotherapy shapes the treatment beam, adapting it to the outline of the tumor. By additionally modulating the fluence of the beam, intensity-modulated radiotherapy (IMRT) improves the dose conformity and spares organs at risk. However, the advantages of these techniques may be compromised by inter- and intrafractional movement of the tumor or adjacent organs at risk.[1] Due to the resulting uncertainty of the target's position the tumor volume may receive an underdosage, whereas healthy tissue may be irradiated undesirably.

In many cancer treatment facilities image-guided radiotherapy (IGRT) is utilized to compensate for interfractional target motion. Hereby, the locations of the tumor and adjacent organs are determined, while the patient is already lying on the treatment couch, by in-room computer tomography (CT) or linac-integrated kilo- and megavoltage cone-beam CT, in either conventional 3D or time-resolved 4D mode.[2,3] Relying on thus gained positional information, the treatment is adapted accordingly.

To compensate for intrafractional motion in real-time, it is necessary to continuously monitor the target. The Calypso System (Varian Medical Systems, Inc., Palo Alto, CA, USA) is able to determine the target's position in real-time by localizing three implanted resonant circuits, the so-called Beacons.[4] A magnetic array, whose position is determined by three infrared (IR) cameras in the treatment room, excites the Beacons from the outside of the body and detects their responses at a rate of 25 Hz. Afterward, a multileaf collimator (MLC) tracking system can adapt the treatment field's shape and position to the target motion by adjusting the MLC's leaves.[5] Another approach to compensate for movement of the patient is the use of a robotic treatment couch tracking system.[6] Hereby the entire patient is moved in order to countersteer target motion. The CyberKnife system (Accuray, Sunnyvale, CA), the only clinically applied tumor tracking system up to now, repositions the entire linac accordingly to the tumor motion.[7] The VERO system (BrainLAB AG, Feldkirchen, Germany and Mitsubishi Heavy Industries, Tokyo, Japan) features a 6 MV linac with a relatively small MLC mounted onto an O-ring gantry. A gimbals system allows pan and tilt rotation of the entire linac-MLC-assembly for tumor tracking.[8]

At DKFZ (German Cancer Research Center, Heidelberg, Germany) a MLC tracking system based on the Siemens 160 MLC (Siemens Healthcare, Erlangen, Germany) has been developed. Motion monitoring was achieved with either a potentiometer, an x-ray imaging system, or the Calypso System.[9–11] A robotic treatment couch tracking system based on the HexaPOD tabletop (Medical Intelligence Medizintechnik, Elekta Group, Schwabmünchen, Germany) integrated with optical motion monitoring has been realized at the University of Würzburg.[12]

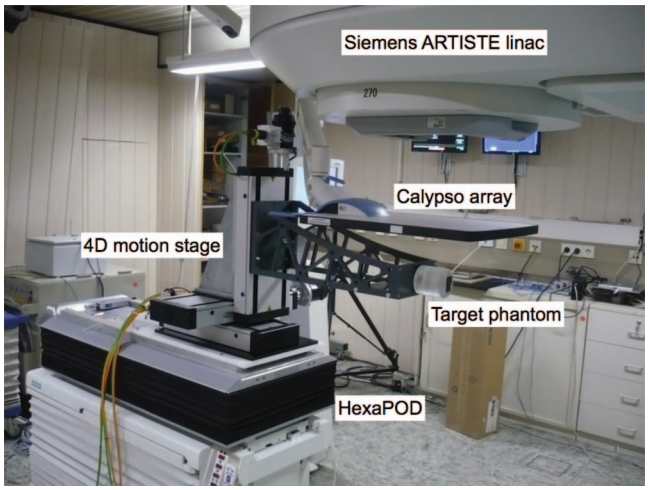

FIG. 1. Photograph of the used experimental setup as used for the determination of the dosimetric accuracy for prostate motion tracking. One can clearly recognize the cylindrical prostate target phantom, which is attached to the base of the 4D motion stage reaching into the treatment field.

In this study, the tracking performances of the two systems were compared under equal conditions. For this, the HexaPOD tracking system has been installed at DKFZ and modified to receive target positions from the Calypso System. The geometric and the dosimetric accuracy of both systems was determined during the tracking of respiratory motion, and furthermore the dosimetric accuracy while compensating for prostate motion was investigated during an IMRT treatment.

II. MATERIALS AND METHODS

II.A. Experimental setup

Figure 1 displays the experimental setup used during this study. The HexaPOD was mounted on top of the Siemens TxT 550 treatment couch. A programmable 4D motion stage, which can reproduce 3D target motion trajectories with submillimeter precision, was fixed to the HexaPOD. For the dose deliveries with tracking by the robotic treatment couch tracking system, the HexaPOD countersteered the movement of the 4D motion stage so that the phantom's position deviated as little as possible from the designated isocenter. During the MLC tracking deliveries the HexaPOD's position was locked.

Two different target phantoms were attached to the base of the 4D motion stage reaching into the treatment field. The first phantom, used for respiratory motion tracking, consists of five stacked solid water slices, each measuring $13 \times 13 \times 1$ cm^3. Three Calypso Beacons were inserted into one slice, allowing localization by the Calypso System. During the tracking of prostate motion, it was replaced by a cylindrical plastic phantom with a diameter of 9 cm and a height of 8.5 cm. Three Calypso Beacons were attached to its surface. Both phantoms were aligned to the isocenter using an in-room laser guidance system. During the organ motion trajectories their positions were continuously determined by the Calypso System with a position accuracy of 0.3 mm and

the information was then reported either to the MLC tracking control system (MTCS) or to the adaptive tumor tracking system (ATTS) of the HexaPOD.

In this study the y axis is pointing from the isocenter toward the gantry, and the z axis is pointing from the isocenter toward the ceiling of the treatment room. For the respiratory motion tracking experiments, the on-board amorphous silicon flat panel detector (40×40 cm^2 with a pixel pitch of 0.4×0.4 mm^2) of the linac was utilized in order to assess the geometric accuracy.

II.B. Tracking systems

II.B.1. The MLC tracking control system

The MTCS adapts the aperture of a Siemens 160 MLC in real-time to target motion continuously monitored by the Calypso System.[11] Due to the finite leaf width, MLC tracking cannot perfectly compensate for target motion perpendicular to the leaf travel direction. Parts of the desired field shape are blocked (underdosage) and areas outside of the desired field are irradiated (overdosage). Our leaf positioning algorithm weights underdosage and overdosage areas equally, optimizing the conformity with the desired translated field shape while maintaining the integral fluence. The first closed leaf pair beside the open field is placed in the middle of the positions of the adjacent open leaf pair to be able to open quickly in case of rapid target motion perpendicular to the leaf travel direction. For respiratory motion tracking, two further closed leaf pairs are retracted by 1 and 5 cm, respectively, to minimize the leakage through leaf tips, which is largest on the central axis.[9] The closing position of the other leaf pairs is at −5.5 cm from the isocenter.

The total latency of the MLC tracking system integrated with the Calypso System amounts to about 0.6 s.[11] In order to guarantee accurate target tracking the total system latency is compensated for by means of target motion forward prediction. We use a support vector regression (SVR) based respiratory motion forward predictor, which performed favorably in a previous prediction model comparison study.[13] The implementation of SVR prediction into the MTCS is based on the C++ package LIBSVM.[14]

We use a common set of SVR prediction model parameters, which were optimized to yield high prediction accuracies for a population of 12 breathing trajectories. Prior to the actual forward prediction step, we have applied data preprocessing to reduce lung tumor motion baseline drifts and fluctuations of the breathing amplitudes as outlined in Ref. 13. After the actual prediction step, the predicted values are backtransformed. Importantly, the preprocessing is not applied to the target motion patterns of the 4D motion stage, but represented only an intermediate step in the prediction procedure to enhance the prediction accuracy.

II.B.2. The adaptive tumor tracking system

Similar to the MTCS, the control system of the ATTS based on the HexaPOD consists of two major components: a predictor forecasting tumor motion and a control scheme computing necessary control inputs to the HexaPOD in order to realize tumor motion compensation by adapting the patient's position.

The standard setup of the ATTS as reported in Ref. 12 was modified to receive tumor position information from the Calypso System, which is calibrated to the HexaPOD reference frame. The position of the HexaPOD is still determined by IR markers with a Polaris Spectra® IR camera (NDI, Waterloo, Ontario, Canada), which is also calibrated to the HexaPOD reference frame. The software package *HexGuide* is triggered by the IR camera at an equidistant rate of 10 Hz. The samples of the Calypso System, arriving at a nonequidistant average rate of about 25.6 Hz with latencies (reported by the Calypso real-time data protocol) up to about 150 ms, are linearly interpolated to the sampling intervals of the trigger. In each sampling instant (shifted back in time accordingly to an estimation of the latency of the IR camera), the current position of the HexaPOD is subtracted from the interpolated Calypso data to deliver the motion relative to the HexaPOD, which is then fed into the predictor. The lag caused by interpolation and the latency of the Calypso System is completely compensated for by dynamically adjusting the prediction horizon, so that exactly a one step-ahead prediction (relative to last sampling instant of the trigger) is available, which is a requirement of the used control method. Effectively, the predictor needs to compute predictions up to a horizon of three samples (300 ms) in this setup.

The employed predictor is based on a finding made by Takens which can be used to reconstruct states of unknown dynamical systems.[15] In each sampling instant, the predictor determines an embedding vector which can be interpreted as some kind of a recent motion pattern, consisting of several past and transformed position measurements of the beacon. This embedding vector is then compared to all other embedding vectors determined in previous sampling instants. From several best matching vectors, the prediction of a future tumor position is determined. Three parameters need to be chosen, determining the dimension of the embedding vectors and number of best matches included in the predictions. These are adapted online according to the current major motion frequency which is permanently estimated. Hence, the predictor starts with no knowledge, where useful predictions can already be obtained after 8–10 s. In order to already achieve motion compensation during this startup time, predictions are replaced by the latest measurement and used as input to the controller. The full prediction method is discussed in more detail in Ref. 16.

After the prediction has been computed, which requires at maximum about 2.567 ms (with an average of 0.390 ms), this latency is compensated for by estimating the current position of the HexaPOD (current in the sense of right at the time after the predictor is finished) based on that latency plus the estimated age of the IR measurement. This current position is then fed into the control method.

The control for the HexaPOD is arranged as an outer control loop around the internal controller of the HexaPOD, computing the control inputs in form of three positions, three

orientations (not used in this work) and one normalized speed value. The control law[17] is based on geometrical properties of the tracking problem in three translational dimensions. In the implementation used in this work it is configured to require only a one-step ahead prediction from which the control input is calculated in such a way that the negated position prediction (assuming the origin of the HexaPOD reference frame was calibrated to the isocenter) is reached by the HexaPOD at the beginning of the next sampling instant.

The computations of the controller take at maximum 0.080 ms (with an average time of 0.025 ms) and the serial transmission time of the control input to the HexaPOD is 9.375 ms (54 bytes at 57 600 bps with 8N1). These latencies of about 10 ms are not compensated for in the current implementation. There is another latency between the reception of the control input on the HexaPOD and the application of the final control input on the motors. This latency is unknown but based on observations of the HexaPOD's behavior during motion assumed to be significantly smaller than the duration of one sampling interval, so that the noncompensated latencies are neglected in this work. In Ref. 17 a detailed experiment is published, demonstrating the validity of negligence of the latencies even with double the update rate of 20 Hz. Any positioning errors resulting from latencies were canceled due to the closed-loop operation of the controller. Tests using this controller on ideal sine trajectories having similar characteristics as tumor motions and defining the reference trajectory to be reached by the HexaPOD, yielded very low tracking errors of less than 0.08 mm at maximum. However, if the reference trajectory is shaped in such a way to exceed the maximum speed of the HexaPOD of 16 cm/s, then tracking errors are to be expected, being proportional to the amount of exceedance. Thus, the overall performance of the ATTS is only limited by the maximum speed and accuracy of predictions.

II.C. Organ motion data

The respiratory motion data used for the geometric and dosimetric comparison of the MLC and the HexaPOD tracking systems was acquired during gated radiotherapy treatments.[18,19] Hereby the internal lung tumor motion was determined by a stereoscopic kilovoltage x-ray system at a frame rate of 30 Hz. The used trajectories were chosen in order to represent a large variety of breathing patterns (cf. Table I). Breathing shape, period length, and peak-to-peak amplitude may vary not only between the different respiratory motion samples, but also over the course of a single session. Additionally, baseline drifts as well as sudden shifts can be observed in several motion samples.

The two motion directions with the largest mean amplitudes were used and translated into y and x movements of the 4D motion stage. All motion data had to be smoothed by a spline fit in order to avoid bucking of the 4D motion stage caused by rapid accelerations and decelerations due to noise-polluted trajectories.

The prostate motion trajectories were measured with the Calypso System during radiotherapy treatments.[20] The selected trajectories exhibited quick positional shifts up to a few centimeter in a couple of seconds as well as slow drifts of several millimeter over the course of several minutes. The selection of trajectories includes a large variety of motions (cf. Table II). The mediolateral, cranial–caudal, and dorsoventral motion was translated into movement along the x, y, and z axes.

TABLE I. Summary of the characteristics of the used breathing trajectories. Shown are the mean amplitude and standard deviation of the displacement in dorsoventral (DV), mediolateral (ML), and cranial–caudal (CC) direction as well as the mean period length of the breathing motions.

Respiratory motion	Mean amplitude (mm)			Standard deviation (mm)			Mean period length (s)
	DV	ML	CC	DV	ML	CC	
1	4.1	3.6	13.7	1.5	1.4	5.7	3.2
2	6.3	1.6	8.2	2.2	0.4	2.9	2.9
3	4.2	2.1	8.5	1.4	0.6	3.0	3.6
4	0.9	1.6	10.1	0.2	0.7	3.8	2.5
5	2.1	1.4	11.6	0.6	0.7	4.0	4.3
6	4.9	2.0	14.0	2.4	1.1	6.8	2.8
7	8.3	2.8	9.2	3.1	1.0	3.1	3.1
8	7.9	3.2	9.1	3.2	1.3	3.8	3.3

II.D. Geometric accuracy for respiratory motion tracking

During the determination of the geometric accuracy, the 4D motion stage followed the given breathing trajectories. The first 30 s of each trajectory were used to train the prediction filter of the MTCS or ATTS. Over the next period of 45 s the radiation beam, forming a circular treatment field of 5 cm in diameter, was turned on while the respective tracking system compensated for the target motion. The MLC's collimator was rotated by 90° in order to align the leaves in cranial–caudal direction, the main motion direction of the breathing trajectories. During the tracking deliveries MV images were continuously acquired by the flat panel detector at a rate of 10 Hz. The positions of a metal marker, inserted into the target phantom at the designated isocenter, and the geometric centroid of the circular MV field were automatically extracted from the portal images using a threshold-based detection algorithm outlined in Ref. 11 (cf. Fig. 2).

TABLE II. Summary of the characteristics of the used prostate motion trajectories.

Prostate motion	Main positional characteristics
1	Several shifts up to 6 mm for 10 s and a gradual baseline drift of 2 mm.
2	Three shifts up to 15 mm for 30 s and a gradual baseline drift of 5 mm.
3	Gradual baseline drift of 3 mm, several small and one large shift of 18 mm for 20 s.
4	Sudden baseline shift of about 8 mm.
5	Gradual baseline drift of 7 mm.

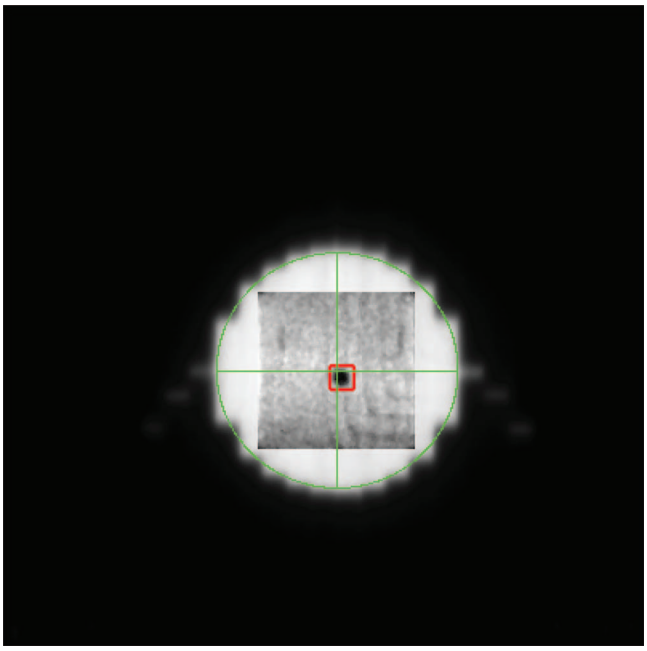

FIG. 2. A MV image of the target phantom containing a metal marker irradiated with a round treatment field with a diameter of 5 cm. After enhancing the contrast in a region of interest the metal pellet marking the target position is clearly recognizable (box). Also, the position of the treatment beam has been determined (circle and cross).

The geometric accuracy of both tracking systems was quantified by measuring the distance between the position of the treatment beam's center and the target in every frame and calculating the root mean square error (RMSE) in x and y directions for the entire tracking procedure.

By plotting the trajectories of the target and the treatment beam, the performance of the MLC tracking system for different target motions was further investigated.

During the deliveries with the HexaPOD tracking system the entire 4D motion stage was moved, resulting in two superimposed motions being observed on the MV images. In order to obtain target and compensation trajectories comparable with those of the MLC tracking system, the log files of the HexaPOD tracking system were read out and the motions were transformed into the patient's coordinate system.

II.E. Dosimetric accuracy for respiratory motion tracking

In order to compare the dosimetric accuracy of the MLC and the HexaPOD tracking system, EDR2 films (Eastman Kodak, Rochester, New York, USA) were inserted into the target phantom at the isocenter parallel to the x–y plane and their positions were marked by three small pin pricks through defined holes within the phantom. The same respiratory motion trajectories as used during the comparison of the geometric accuracy were simulated by the 4D motion stage and compensated for by the respective tracking systems. Again, the first 30 s of the breathing trajectories were used to train the prediction filter of the MTCS or ATTS. During the following period of 45 s the films were irradiated with 225 MU through a circular treatment field with a diameter of 5 cm. Also films without target motion compensation and a static film as a reference were irradiated.

The deviations of the dose distributions on the moved films from that on the static film were quantified by means of the 2%/2 mm local difference gamma criterion while suppressing dose values below 5% of the maximum dose.

II.F. Dosimetric accuracy for prostate motion tracking

During the determination of the dosimetric accuracy of the tracking systems for prostate motion tracking, EDR2 films were inserted into the cylindrical target phantom parallel to the y–z plane and marked by three pin pricks at defined positions. They were then irradiated with 65 segments from 7 beam angles during a 9 m long step-and-shoot IMRT treatment. The treatment was based on CT images of the cylindrical target phantom and optimized to deliver a maximum dose to a prostate tumor while sparing the rectum. The leaves of the MLC were aligned perpendicular to the cranial–caudal direction. The prostate motion trajectories were reproduced by the 4D motion stage. During irradiation of the films, the target motion was compensated for by both tracking systems. However, the predictors of the MTCS and the ATTS were not used due to the irregularity of prostate motion compared to respiratory motion. Thus, the latest position measurement replaces the prediction. Also films without motion compensation and a static film as a reference were irradiated.

By determining the deviations of the dose distribution on the moved films from that on the statically irradiated film by means of the 2%/2 mm gamma criterion, we have quantified the improvement of the treatment.

III. RESULTS

III.A. Geometric accuracy for respiratory motion tracking

Figure 3 displays the RMSE in x and y directions, respectively, with and without compensation of the respiratory motion by the tracking systems. Without tracking the RMSE varied strongly. The MLC as well as the HexaPOD tracking system reduced the RMSE in all cases, but the RMSE still differed strongly for the different breathing trajectories. Also, the relative reduction of the RMSE varied depending on the breathing trajectory.

Averaged over all considered breathing trajectories, the MLC as well as the HexaPOD tracking system approximately halved the RMSE compared to no tracking method used, with only small differences being observed between motion parallel or perpendicular to the leaf direction. The average RMSE in y direction was reduced from 4.1 to 2.0 mm and to 2.2 mm for the MLC and HexaPOD tracking systems, respectively. In x direction it was reduced from 1.9 to 0.9 mm by the MLC tracking system and to 1.0 mm by the HexaPOD tracking system.

The successful tracking of breathing trajectory 6 in y direction is shown in Fig. 4. Although the mean amplitude changed

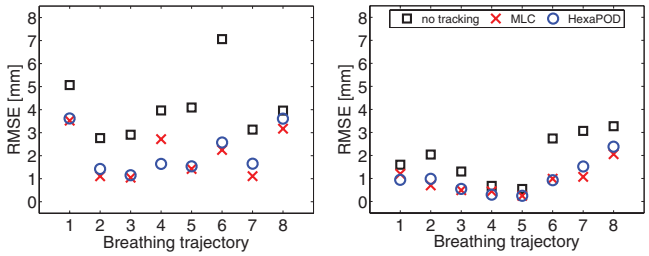

FIG. 3. Geometric root mean squared tracking errors in (a) x direction and (b) y direction for the different breathing trajectories and tracking methods.

and the target drifted over the course of the tracking, the MLC as well as the HexaPOD tracking system were able to follow the target motion accurately, reducing the RMSE by 68% and 63%, respectively.

The problematic tracking of breathing trajectory 8 in y direction is shown in Fig. 5. The intense ex- and inhaling by the patient at second 40 resulted in a doubling of the amplitude and period for one breathing cycle. Both tracking systems were unable to track the sudden alternation of the breathing motion. Afterward, the MLC tracking control system adapted quicker to the again regular respiratory motion and was able to track the following breathing cycle. The adaptive tumor tracking system needed an extra period to adapt. Because of these difficulties the HexaPOD tracking system reduced the RMSE for this trajectory only by 10% and the MLC tracking system only by 20%.

III.B. Dosimetric accuracy for respiratory motion tracking

The 2%/2 mm gamma success rates with and without respiratory motion compensation are shown in Fig. 6. The HexaPOD tracking system outperformed the MLC tracking system for every breathing trajectory. Depending on the compensated respiratory motion trajectory, its gamma pass rate was at least 0.2% and up to 17.0% higher, averaging at 5.5%. The improvements of MLC tracking compared to no motion compensation were small for breathing trajectories 1–3. For trajectories 4–8, both tracking methods improved the dosimetric accuracy substantially. The 2%/2 mm gamma passing rates averaged over all breathing trajectories were 76.4%, 89.8%, and 95.3% for no tracking, the MLC, and the HexaPOD tracking systems, respectively.

The dose distributions with and without motion compensation of breathing trajectory 6 are displayed in Fig. 7. The 2%/2 mm gamma success rate was increased from 47.0% without tracking to 92.3% and 97.6% for the MLC and HexaPOD tracking systems, respectively. For MLC tracking, overdosed regions could be observed adjacent to the left and right sides of the high dose area. These areas were present on the dose distributions of every breathing trajectory compensated for by the MLC tracking system, but not on dose distributions acquired during motion compensation with the HexaPOD tracking system.

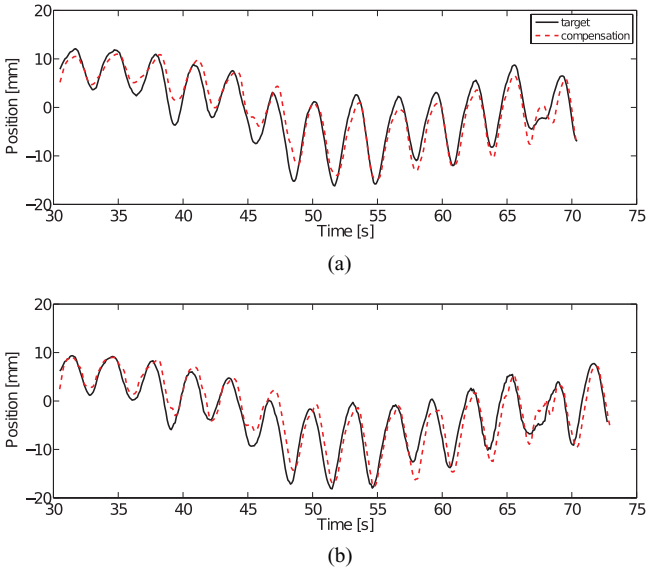

FIG. 4. (a) The MLC and (b) HexaPOD tracking system compensating the y motion of breathing trajectory 6. Compensation represents the treatment beam's position for MLC tracking and the patient couch's position contrary to the target motion for HexaPOD tracking.

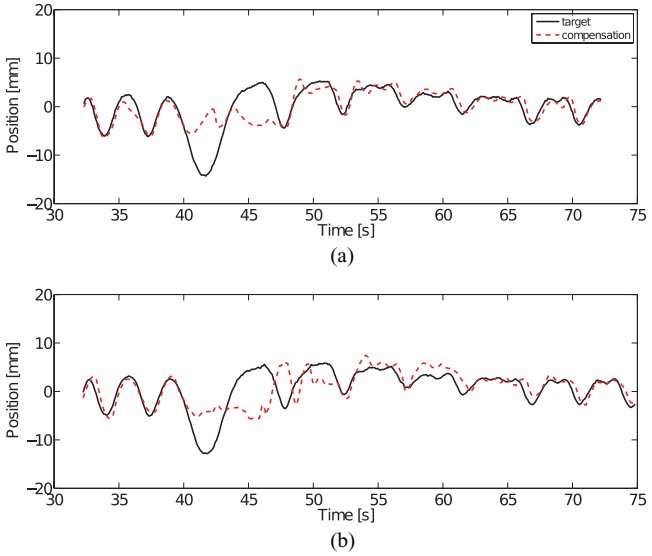

FIG. 5. (a) The MLC and (b) HexaPOD tracking systems compensating the y motion of breathing trajectory 8. Compensation represents the treatment beam's position for MLC tracking and the patient couch's position contrary to the target motion for HexaPOD tracking.

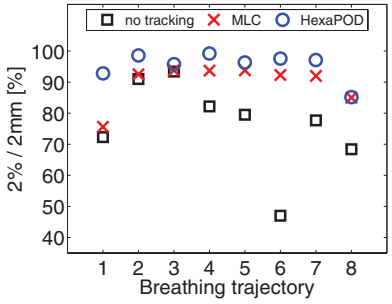

FIG. 6. Amount of points passing the 2%/2 mm gamma criterion depending on the different breathing trajectories and tracking methods.

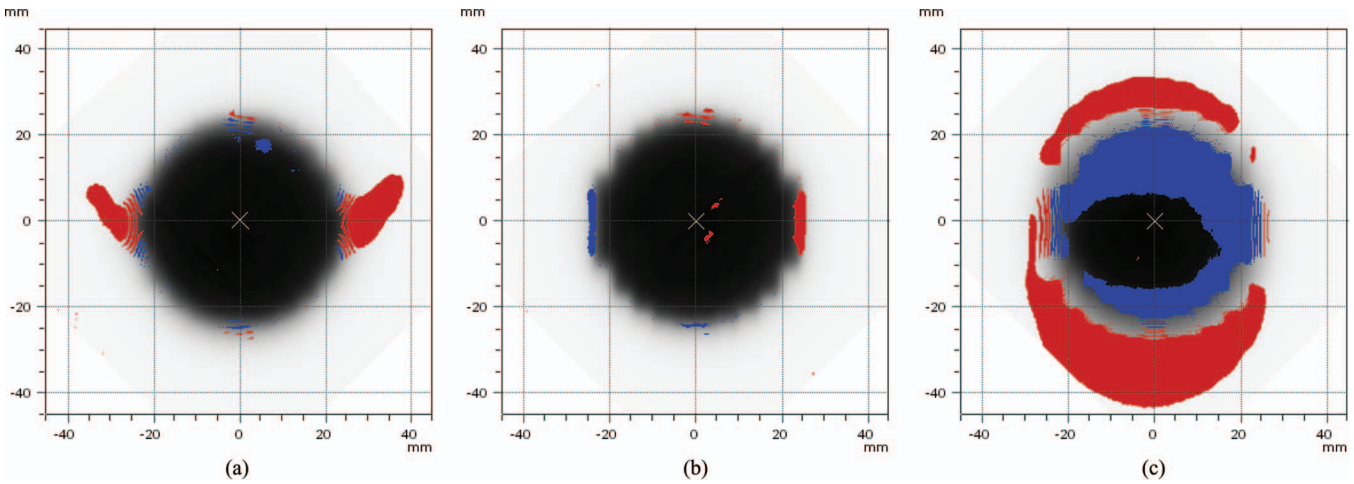

FIG. 7. Grayscale dose distributions for (a) MLC tracking, (b) HexaPOD tracking, and (c) without tracking compensating breathing trajectory 6. Red areas represent an overdosage and blue areas an underdosage regarding a 2%/2 mm gamma index >1. The vertical axis of the film is parallel to the leaf direction of the MLC and the *y* axis in the treatment room coordinates.

III.C. Dosimetric accuracy for prostate motion tracking

Figure 8 displays the 2%/2 mm gamma success rates for the different prostate motion trajectories and compensation methods. Both tracking systems increased the amount of points passing the gamma criterion. However, the compensation ability of the MLC tracking system lagged behind the HexaPOD tracking system for every prostate motion trajectory. While the HexaPOD tracking system increased the gamma success rate to 95.3% in average, the average amount of points passing for MLC tracking was 85.0%, lagging behind by a 10.3% worse gamma pass rate on average, spanning between 3.5% and 25% worse gamma pass rates. The MLC tracking system's accuracy for prostate motion trajectories 2 and 4 was clearly worse than for the others. Without motion compensation on average only 60.1% of the points passed the gamma criterion.

The dose distributions for the different tracking methods for prostate motion 2 are shown in Fig. 9. For MLC as well as HexaPOD tracking, over- as well as underdosed areas appeared primarily on the edges parallel to the leaf direction. The amount of points passing the 2%/2 mm gamma criterion was increased from 45.8% to 95.0% by the HexaPOD tracking system and to 82.0% by the MLC tracking system.

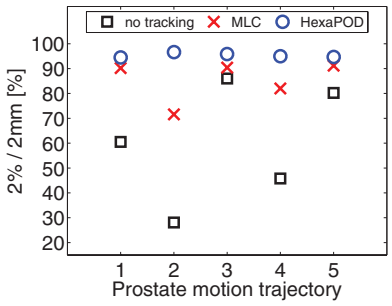

FIG. 8. Amount of points passing the 2%/2 mm gamma criterion for the different prostate motion trajectories and tracking methods.

IV. DISCUSSION

In this work the performances of the MLC tracking system based on the adaption of the treatment beam with a dynamic MLC and the HexaPOD tracking system repositioning the entire patient with a robotic treatment couch have been compared. Both tracking systems received continuous target position updates from the Calypso System. The tracking performance has been assessed for eight respiratory and five prostate motion trajectories.

During respiratory motion both tracking systems roughly halved the geometric RMSE compared to deliveries without motion compensation. For the MLC tracking system, the remaining errors were predominantly caused by prediction errors and not by physical limitations of the tracking system such as maximum leaf acceleration or velocity. The dynamic MTCS log files of the geometric tracking accuracy measurements contain target positions as reported by the Calypso System as well as forward predictions of the target positions. Prediction errors could therefore be calculated from the log files. The RMS prediction errors averaged over the eight breathing trajectories were 0.85 mm in *x* direction and 1.97 mm in *y* direction; this corresponds to 94% and 98% of the respective geometric tracking errors determined from the MV images. During MLC tracking the outlines of the treatment field perpendicular to the movement direction of the leaves cannot have a better resolution than the leaf width. However, the geometric centroid of the treatment field does not have this limitation as it shifts continuously as leaf pairs at the edge of the treatment field are gradually opened or closed. As we measure the position of the geometric centroid during the assessment of the root mean square error, the measurement of the geometric accuracy is not limited by the leaf width.[9,21]

The remaining errors of the HexaPOD tracking system also seemed to be caused by the predictor and not by couch travel speed or acceleration limitations as the largest tracking errors did not occur for the compensation of breathing trajectory 6 with the fastest and largest target motion, but on breathing

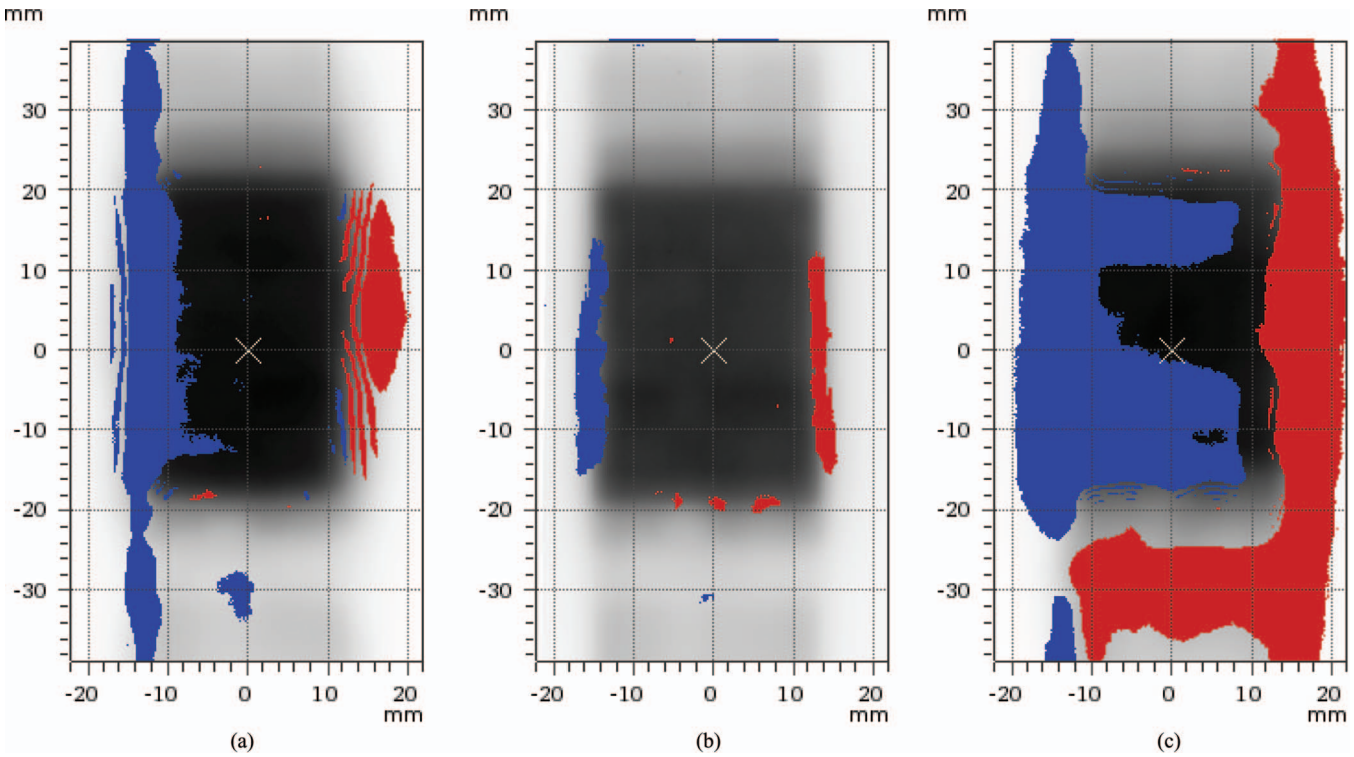

FIG. 9. Grayscale dose distributions for (a) MLC tracking, (b) HexaPOD tracking, and (c) without tracking compensating prostate motion trajectory 2. Red areas represent an overdosage and blue areas an underdosage regarding a 2%/2 mm gamma index >1. The vertical axis of the film is parallel to the leaf direction of the MLC and to the z axis in the treatment room coordinates.

trajectories 1 and 8, which exhibited sudden changes of the breathing pattern.

In spite of the almost equal geometric accuracy of the MLC tracking system, the HexaPOD tracking system yielded a better dosimetric accuracy for the respiratory motion compensation; especially for respiratory motion trajectories 1–3, during which the MLC tracking system was only barely able to improve the dosimetric accuracy. The dosimetric accuracy of the MLC tracking system is mainly reduced by two issues: First, the finite leaf width of 5 mm, as the MTCS has to decide whether to open or not to open an additional leaf pair during movement perpendicular to the leaf direction. Second, leakage through closed leaf pairs, which have to be positioned adjacent to open leaf pairs to be able to quickly open in case of target motion perpendicular to the leaf travel direction. By constantly changing this storage position (feathering technique[22]) or completely relinquishing these closed leaf pairs, one could distribute the interleaf leakage more evenly or decrease it. However, both these approaches come at cost of a worse tracking accuracy of motion perpendicular to leaf direction.

The HexaPOD outperformed the MLC even more clearly for the dosimetric accuracy evaluation during prostate motion. Prostate motion typically exhibits slow drifts over the entire course of a radiotherapy fraction. Roughly constant target position offsets of several millimeters are often observed during the delivery of individual IMRT segments or even entire beams. Tracking errors due to the finite leaf width cannot average out during MLC tracking and are therefore more pronounced than for respiratory motion tracking.

Another reason is the reduced latency of the ATTS. Since this system was configured for prostate motion compensation to use the latest interpolated Calypso measurement (interpolated to a sampling rate of 10 Hz) instead of the one-step ahead prediction as a set-point for the next sampling instant, the measurement- and interpolation-induced latency in this scenario is exactly either 200, 300, or at maximum 400 ms, depending on the age of the corresponding Calypso measurement (assuming the age is less than 200 ms), compared to a total system latency of 600 ms of the MLC tracking system. The latency of the ATTS could be further reduced by increasing the sampling rate of the trigger to about 20 Hz as this latency is a multiple of the sampling period. However, a small improvement of the tracking error, which could be gained by an increased sampling rate, was sacrificed in favor of smoother trajectories to account for increased patient comfort.

The experimental methodology with the use of rigid target phantoms did not account for the following concerns associated with robotic treatment couch tracking applied to rapid respiratory motion: First, patient comfort might be compromised. Second, couch motion might be different from organ motion due to potential patient anatomy deformation in response to the couch acceleration. It has been reported that couch tracking of respiratory motion was tolerated well by a group of patients and volunteers.[23,24] Also, no significant changes within the breathing patterns for couch tracking were observed. To our knowledge, the possibility of acceleration induced patient anatomy deformation has not yet been investigated.

Unlike the tumor tracking systems based on the HexaPOD and the Siemens 160 MLC featured in this work, the CyberKnife and VERO tracking systems have been specifically designed to compensate for intrafractional organ motion in real-time, circumventing some of the observed difficulties experienced with the MLC and HexaPOD tracking systems.

Compared to the tracking systems utilized in this work, both systems have lower system latencies of 0.12 and 0.05 s, respectively, resulting in a higher geometric accuracy.[25,26] Furthermore, the patient's position remains stationary during the treatment with the CyberKnife or VERO system. Therefore, these systems will not have any impact on patient stability, anatomy, or comfort. However, the field size of the VERO system is relatively small, which limits its possible fields of application. The CyberKnife system is not equipped with a MLC and the delivery times are often substantially larger compared to radiotherapy deliveries with a medical x-ray producing linac. Additionally, MLC tracking or motion compensation with a robotic treatment couch could be advantageous from an economical point of view. Medical x-ray producing linacs equipped with MLCs are the "working horses" of modern radiotherapy. MLC tracking essentially only requires software modifications and HexaPOD tracking requires the installation of a new treatment couch, so that both have the potential for a relatively cost-effective, widespread clinical implementation.

V. CONCLUSION

To our knowledge this paper presents the first direct comparison of a tracking system based on a robotic treatment couch and a MLC tracking system. In the course of the work, the geometric tracking accuracy was increased almost equally for both systems. Also, both systems yielded a substantially improved dosimetric accuracy compared to the deliveries without motion compensation. The performance comparison showed a superior dosimetric tracking accuracy for the HexaPOD tracking system for the considered organ motion trajectories. The dosimetric disadvantage of the MLC tracking system is predominantly caused by the hardware limitations of the MLC; namely, the leaf width of 5 mm and leakage through the closed leaf pairs. There are concerns associated with rapid patient motion induced by couch tracking of respiratory motion; MLC tracking might therefore be the preferred method for respiratory motion tracking in spite of the slightly inferior dosimetric accuracy. For slow prostate motion compensation, the obtained data suggest that HexaPOD tracking is clearly favorable.

However, we feel that both used systems can be further improved and tested under more realistic experimental conditions as well as the respective tracking systems can be compared to systems of the same type.

ACKNOWLEDGMENTS

The authors would like to thank Torben Mersebach, Werner Sanktjohanser, and Guido Kübler from Guido Kübler GmbH, Bobingen, Germany for the provision and setup of the HexaPOD as well as Gernot Echner and Armin Runz for their mechanical help setting up the experiment. This work was partially supported by Siemens Healthcare and Calypso Medical Technologies and a grant from the Bavarian Research Foundation (BFS).

[a]Electronic mail: m.menten@dkfz.de

[1]T. Bortfeld, S. B. Jiang, and E. Rietzel, "Effects of motion on the total dose distribution," Semin. Radiat. Oncol. **14**, 41–51 (2004).
[2]D. Jaffray, P. Kupelian, T. Djemil, and R. M. Macklis, "Review of image-guided radiation therapy," Expert Rev. Anti-cancer Ther. **7**, 89–103 (2007).
[3]J.-J. Sonke, L. Zijp, P. Remeijer, and M. van Herk, "Respiratory correlated cone beam CT," Med. Phys. **32**, 1176–1186 (2005).
[4]J. M. Balter, J. N. Wright, L. J. Newell, B. Friemel, S. Dimmer, Y. Cheng, J. Wong, E. Vertatschitsch, and T. P. Mate, "Accuracy of a wireless localization system for radiotherapy," Int. J. Radiat. Oncol. Biol. Phys. **61**, 933–937 (2005).
[5]P. J. Keall, H. Cattell, D. Pokhrel, S. Dieterich, K. H. Wong, M. J. Murphy, S. S. Vedam, K. Wijesooriya, and R. Mohan, "Geometric accuracy of a real-time target tracking system with dynamic multileaf collimator tracking system," Int. J. Radiat. Oncol. Biol. Phys. **65**, 1579–1584 (2006).
[6]W. D. D'Souza and T. J. McAvoy, "An analysis of the treatment couch and control system dynamics for respiration-induced motion compensation," Med. Phys. **33**, 4701–4709 (2006).
[7]A. Schweikard, H. Shiomi, and J. Adler, "Respiration tracking in radiosurgery," Med. Phys. **31**, 2738–2741 (2004).
[8]K. Takayama, T. Mizowaki, M. Kokubo, N. Kawada, H. Nakayama, Y. Narita, K. Nagano, Y. Kamino, and M. Hiraoka, "Initial validations for pursuing irradiation using a gimbals tracking system," Radiother. Oncol. **93**, 45–49 (2009).
[9]M. B. Tacke, S. Nill, A. Krauss, and U. Oelfke, "Real-time tumor tracking: automatic compensation of target motion using the Siemens 160 MLC," Med. Phys. **37**, 753–761 (2010).
[10]M. F. Fast, A. Krauss, U. Oelfke, and S. Nill, "Position detection accuracy of a novel linac-mounted intrafractional x-ray imaging system," Med. Phys. **39**, 109–118 (2012).
[11]A. Krauss, S. Nill, M. Tacke, and U. Oelfke, "Electromagnetic real-time tumor position monitoring and dynamic multileaf collimator tracking using a Siemens 160 MLC: geometric and dosimetric accuracy of an integrated system," Int. J. Radiat. Oncol. Biol. Phys. **79**, 579–587 (2011).
[12]J. Wilbert, J. Meyer, K. Baier, M. Guckenberger, C. Herrmann, R. Hefl, C. Janka, L. Ma, T. Mersebach, A. Richter, M. Roth, K. Schilling, and M. Flentje, "Tumor tracking and motion compensation with an adaptive tumor tracking system (ATTS): system description and prototype testing," Med. Phys. **35**, 3911–3921 (2008).
[13]A. Krauss, S. Nill, and U. Oelfke, "The comparative performance of four respiratory motion predictors for real-time tumour tracking," Phys. Med. Biol. **56**, 5303–5317 (2011).
[14]C.-C. Chang and C.-J. Lin, "LIBSVM: a library for support vector machines," http://www.csie.ntu.edu.tw/~cjlin/libsvm/.
[15]F. Takens, *Dynamical Systems and Turbulence, Warwick 1980*, Lecture Notes in Mathematics Vol. 898, edited by D. Rand, and L.-S. Young (Springer, Berlin, 1981), pp. 366–381.
[16]L. Ma, C. Herrmann, and K. Schilling, in *Proceedings of the 2007 IEEE/RSJ International Conference on Intelligent Robots and Systems (IROS 2007)* (IEEE, San Diego, CA, 2007), pp. 189–194.
[17]C. Herrmann, L. Ma, J. Wilbert, K. Baier, and K. Schilling, "Control of a HexaPOD treatment couch for robot-assisted radiotherapy," Biomed. Eng./Biomed. Tech. (accepted).
[18]Y. Seppenwoolde, H. Shirato, K. Kitamura, S. Shimizu, M. van Herk, J. V. Lebesque, and K. Miyasaka, "Precise and real-time measurement of 3D tumor motion in lung due to breathing and heartbeat, measured during radiotherapy," Int. J. Radiat. Oncol. Biol. Phys. **53**, 822–834 (2002).
[19]R. Berbeco, S. Nishioka, H. Shirato, G. T. Y. Chen, and S. B. Jiang, "Residual motion of lung tumours in gated radiotherapy with external respiratory surrogates," Phys. Med. Biol. **50**, 3655–3667 (2005).
[20]D. Schmitt, S. Nill, K. Herfarth, M. Münter, J. Pfitzenmaier, A. Z. du Bois, F. Röder, P. Huber, and U. Oelfke, "Intrafraction Organ Motion during Prostate Radiotherapy: Quantitative Correlation of Treatment Time and Margin Size," Int. J. Radiat. Oncol. Biol. Phys. **78**, 752 (2010).

[21]P. Poulsen, B. Cho, A. Sawant, D. Ruan, and P. Keall, "Dynamic MLC tracking of moving targets with a single kV imager for 3D conformal and IMRT treatments," Acta Oncol. **49**, 1092–1100 (2010).
[22]B. Y. Yi, S. Han-Oh, F. Lerma, B. L. Berman, and C. Yu, "Real-time tumor tracking with preprogrammed dynamic multileaf-collimator motion and adaptive dose-rate regulation," Med. Phys. **35**, 3955–3962 (2008).
[23]W. D. D'Souza, K. T. Malinowski, S. Van Liew, G. D'Souza, K. Asbury, T. J. McAvoy, M. Suntharalingam, and W. F. Regine, "Investigation of motion sickness and inertial stability on a moving couch for intra-fraction motion compensation," Acta Oncol. **48**, 1198–1203 (2009).
[24]J. Wilbert, K. Baier, A. Richter, C. Herrmann, L. Ma, M. Flentje, and M. Guckenberger, "Influence of continuous table motion on patient breathing patterns," Int. J. Radiat. Oncol. Biol. Phys. **77**, 622–629 (2010).
[25]M. Hoogeman, J.-B. Prévost, J. Nuyttens, J. Pöll, P. Levendag, and B. Heijmen, "Clinical accuracy of the respiratory tumor tracking system of the cyberknife: assessment by analysis of log files," Int. J. Radiat. Oncol. Biol. Phys. **74**, 297–303 (2009).
[26]T. Depuydt, D. Verellen, O. Haas, T. Gevaert, N. Linthout, M. Duchateau, K. Tournel, T. Reynders, K. Leysen, M. Hoogeman, G. Storme, and M. D. Ridder, "Geometric accuracy of a novel gimbals based radiation therapy tumor tracking system," Radiother. Oncol. **98**, 365–372 (2011).